

## Annealing behavior of open spaces in AION films studied by monoenergetic positron beams

Akira Uedono, Takahiro Yamada, Takuji Hosoi, Werner Egger, Tönjes Koschine, Christoph Hugenschmidt, Marcel Dickmann, and Heiji Watanabe

Citation: *Appl. Phys. Lett.* **112**, 182103 (2018); doi: 10.1063/1.5027257

View online: <https://doi.org/10.1063/1.5027257>

View Table of Contents: <http://aip.scitation.org/toc/apl/112/18>

Published by the [American Institute of Physics](#)

---

### Articles you may be interested in

[Correlation between dislocations and leakage current of p-n diodes on a free-standing GaN substrate](#)  
*Applied Physics Letters* **112**, 182106 (2018); 10.1063/1.5024704

[Polarization-induced hole doping in N-polar III-nitride LED grown by metalorganic chemical vapor deposition](#)  
*Applied Physics Letters* **112**, 182104 (2018); 10.1063/1.5023521

[Ultraviolet micro-Raman stress map of polycrystalline diamond grown selectively on silicon substrates using chemical vapor deposition](#)  
*Applied Physics Letters* **112**, 181907 (2018); 10.1063/1.5027507

[Vacancy-type defects in Al<sub>2</sub>O<sub>3</sub>/GaN structure probed by monoenergetic positron beams](#)  
*Journal of Applied Physics* **123**, 155302 (2018); 10.1063/1.5026831

[Integrating AlInN interlayers into InGaN/GaN multiple quantum wells for enhanced green emission](#)  
*Applied Physics Letters* **112**, 201106 (2018); 10.1063/1.5028257

[Large electron capture-cross-section of the major nonradiative recombination centers in Mg-doped GaN epilayers grown on a GaN substrate](#)  
*Applied Physics Letters* **112**, 211901 (2018); 10.1063/1.5030645

---



**Sensors, Controllers, Monitors**  
from the world leader in cryogenic thermometry



## Annealing behavior of open spaces in AlON films studied by monoenergetic positron beams

Akira Uedono,<sup>1</sup> Takahiro Yamada,<sup>2</sup> Takuji Hosoi,<sup>2</sup> Werner Egger,<sup>3</sup> Tönjes Koschine,<sup>3</sup> Christoph Hugenschmidt,<sup>4</sup> Marcel Dickmann,<sup>4</sup> and Heiji Watanabe<sup>2</sup>

<sup>1</sup>Division of Applied Physics, Faculty of Pure and Applied Science, University of Tsukuba, Tsukuba, Ibaraki 305-8573, Japan

<sup>2</sup>Graduate School of Engineering, Osaka University, Suita, Osaka 565-0871, Japan

<sup>3</sup>Institut für Angewandte Physik und Messtechnik, Universität der Bundeswehr München, 85577 Neubiberg, Germany

<sup>4</sup>Physics Department E21 and Heinz Maier-Leibnitz Zentrum (MLZ), Technische Universität München, 85748 Garching, Germany

(Received 28 February 2018; accepted 18 April 2018; published online 3 May 2018)

The impact of nitridation on open spaces in thin AlON<sub>x</sub> films deposited by a reactive sputtering technique was studied by using monoenergetic positron beams. For AlON<sub>x</sub> films with  $x = 0\%–15\%$ , positrons were found to annihilate from trapped states in open spaces, which coexist intrinsically in an amorphous structure with three different sizes. Nitrogen incorporation into the Al<sub>2</sub>O<sub>3</sub> film increased the size of the open spaces, and their density increased as the post-deposition annealing temperature increased. The effect of nitrogen incorporation, however, diminished at  $x = 25\%$ . The observed change in the network structure was associated with the formation of a stable amorphous structure, which we could relate to the electrical properties of AlON<sub>x</sub>/SiO<sub>2</sub>/Si gate stacks.

Published by AIP Publishing. <https://doi.org/10.1063/1.5027257>

Aluminum oxide (Al<sub>2</sub>O<sub>3</sub>) has been extensively studied for the application as gate insulators of metal-oxide-semiconductor field-effect transistors (MOSFETs) because of its beneficial physical properties such as a large dielectric constant, large bandgap, and good adhesion.<sup>1</sup> In particular, Al<sub>2</sub>O<sub>3</sub> is an ideal insulator for wide-gap semiconductors due to an appropriate band offset at the insulator/semiconductor interface.<sup>2</sup> Compared with conventional gate oxides, such as SiO<sub>2</sub> and SiON, however, the amorphous Al<sub>2</sub>O<sub>3</sub> film tends to crystallize after annealing treatments ( $\cong 800^\circ\text{C}$ ).<sup>1,3</sup> This is one of the major concerns for Al<sub>2</sub>O<sub>3</sub> gate insulators because grain boundaries act as a leakage path between semiconductors and electrodes. Another concern is the presence of high density fixed charges in the Al<sub>2</sub>O<sub>3</sub> film and/or the Al<sub>2</sub>O<sub>3</sub>/semiconductor interface. It was reported that nitrogen incorporation into Al<sub>2</sub>O<sub>3</sub> improves the electrical properties of MOSFETs.<sup>4–6</sup> Although the benefits of nitridation are clear, only limited information is available regarding the effects of nitrogen incorporation on the matrix structure of amorphous Al<sub>2</sub>O<sub>3</sub>, which could affect the dielectric constant and electrical properties on gate stacks. Positron annihilation is an established technique for investigating vacancy-type defects and open spaces in crystalline and amorphous materials.<sup>7,8</sup> In the present study, we used this technique to study the effect of nitridation on open spaces in amorphous Al<sub>2</sub>O<sub>3</sub> films.

The substrate used in this study was Si(100) wafer, on which SiO<sub>2</sub> films (8 nm thick) were grown by thermal oxidation. 10 nm thick AlON<sub>x</sub> ( $x = 0\%–25\%$ ) films were deposited on the SiO<sub>2</sub>/Si template at room temperature by using a reactive sputtering technique with an Al target. Details on the deposition conditions are given elsewhere.<sup>5,9</sup> AlON<sub>x</sub> and Al<sub>2</sub>O<sub>3</sub> depositions were performed in N<sub>2</sub>/O<sub>2</sub> and Ar/O<sub>2</sub> gas mixtures, respectively. The AlON<sub>x</sub> films with different nitrogen contents were prepared by controlling O<sub>2</sub> partial pressure

during the deposition. After the deposition, they were annealed at temperature ranging from 600 °C to 900 °C for 3 min in the N<sub>2</sub> atmosphere. The nitrogen content in the AlON<sub>x</sub> film was estimated by x-ray photoelectron spectroscopy (PHI Quantera SXM, ULVAC-PHI). For electrical measurements, circular Ni gate electrodes with 100 μm diameter and Al back contacts were formed by vacuum evaporation to fabricate AlON<sub>x</sub>/SiO<sub>2</sub>/Si MOS capacitors. The *C*-*V* characteristics were measured at a frequency of 1 MHz using an Agilent B1500A semiconductor device parameter analyzer. The flat-band voltage,  $V_{fb}$ , was estimated using the calculated flat-band capacitance.

Details on the positron annihilation technique are given elsewhere.<sup>7,8</sup> In the present experiments, the Doppler broadening spectra of the annihilation radiation were measured with a Ge detector as a function of the incident positron energy *E*. The energy resolution of the detector was 1.2 keV (full width at half maximum, FWHM), and the counting rate was about 1000 s<sup>-1</sup>. The spectra were characterized by the *S* parameter, defined as the fraction of annihilation events in the energy range of 510.24–511.76 keV. The relationship between *S* and *E* was analyzed by VEPFIT, a computer program developed by van Veen *et al.*<sup>10</sup> The positron lifetime spectrum was measured by using a pulsed monoenergetic positron beam at the NEPOMUC positron source of the Technische Universität München.<sup>11</sup> The lifetime spectrum  $S_{LT}(t)$  is given by  $S_{LT}(t) = \sum (1/\tau_i) I_i \exp(-t/\tau_i)$ , where  $\tau_i$  and  $I_i$  are the positron lifetime and intensity of the *i*-th component, respectively ( $\sum I_i = 1$ ). Approximately  $4 \times 10^6$  counts were accumulated in each spectrum, and the spectra were analyzed with a time resolution of about 200 ps (FWHM) by using the RESOLUTION computer program.<sup>12</sup>

Figure 1 shows the annealing behaviors of  $V_{fb}$  for the AlON<sub>x</sub>/SiO<sub>2</sub>/Si samples with  $x = 0\%$ , 7%, and 25%. The  $V_{fb}$  value was determined from multiple measurements for each

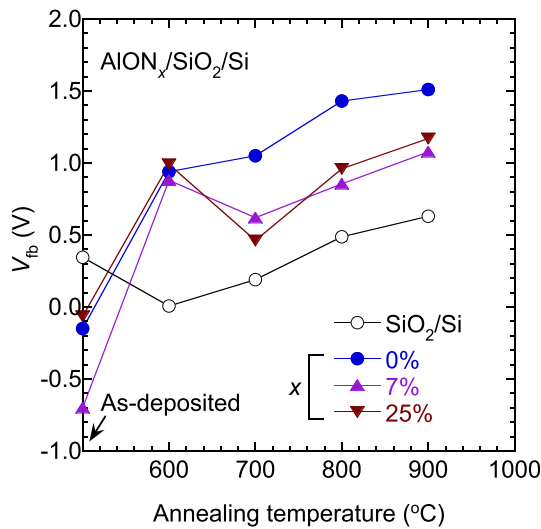


FIG. 1. Flat band voltage  $V_{fb}$  for  $\text{AlON}_x/\text{SiO}_2/\text{Si}$  ( $x = 0\%$ ,  $7\%$ , and  $25\%$ ) as a function of annealing temperature. The result for the  $\text{SiO}_2/\text{Si}$  template is also shown.

sample, and its variation was less than  $\pm 0.05$  V. For the  $\text{SiO}_2/\text{Si}$  template, the value of  $V_{fb}$  kept almost positive (0–0.6 V), and the  $V_{fb}$  shift was small compared with that for  $\text{AlON}_x/\text{SiO}_2/\text{Si}$ . The change in the threshold voltage,  $V_{th}$ , for high- $k$ /metal gate has been explained by the formation of electric dipoles at the high- $k$ /SiO<sub>2</sub> interface.<sup>13,14</sup> For  $\text{Al}_2\text{O}_3/\text{SiO}_2/\text{Si}$ , it is known that the  $V_{th}$  shift due to the dipoles is positive and that the  $V_{th}$  value is stable before and after annealing treatment. Negative charges introduced in  $\text{AlON}_x$  or at the  $\text{AlON}_x/\text{SiO}_2$  interface could also cause the positive shift of  $V_{fb}$ . The  $V_{fb}$  values for  $\text{AlON}_x$  were smaller than those for the sample without nitridation, suggesting that the nitrogen incorporation suppressed the introduction of electric dipoles and/or negative charges.

Figure 2 shows the  $S$  values for  $\text{AlON}_{0.07}/\text{SiO}_2/\text{Si}$  before and after annealing as a function of  $E$ . The statistical error of the  $S$  value is smaller than the size of symbols in the figure. For the as-deposited samples, the  $S$  value increases as  $E$  increases, and it saturates above  $E = 10$  keV. The saturated value coincides with the  $S$  value for the Si substrate (0.531), indicating that almost all positrons annihilated in the Si substrate in this energy range. The mean implantation depth of positrons at

$E = 1$  keV corresponds to the depth of the  $\text{AlON}_{0.07}/\text{SiO}_2$  interface in  $\text{AlON}_{0.07}/\text{SiO}_2/\text{Si}$  and to the  $\text{SiO}_2/\text{Si}$  interface in the template. Therefore, the observed decrease in the  $S$  value at a low  $E$  can be attributed to the annihilation of positrons in the  $\text{AlON}_{0.07}$  film and/or the  $\text{SiO}_2$  films.

For  $\text{AlON}_{0.07}/\text{SiO}_2/\text{Si}$  after annealing, the  $S$  values above  $E = 1$  keV were smaller than those for the as-deposited samples. The diffusion of positrons is affected by the electric field in the depletion region in the Si substrate. The observed decrease in the  $S$  value, therefore, indicates the enhanced diffusion of positrons toward the insulators due to the band bending in Si. This fact agrees well with the  $V_{fb}$  shift shown in Fig. 1. The obtained  $S$ - $E$  curves were analyzed by using the VEPFIT code, and the solid curves in Fig. 2 are fits to the experimental data. In the fitting, the region sampled by positrons was divided into four blocks. Here, the first and second blocks correspond to the annihilation of positrons in the  $\text{AlON}_{0.07}$  film, and the third and fourth blocks correspond to the annihilation of positrons in the  $\text{SiO}_2$  film and Si substrate, respectively. From the fitting results, it is concluded that the  $S$  value at  $E \cong 0.5$  keV can be attributed to the annihilation of positrons in the  $\text{AlON}_{0.07}$  film.

The annealing behaviors of  $S$  for  $\text{AlON}_x$  with  $x = 0\%$ – $25\%$  are summarized in Fig. 3, where the  $S$  value was averaged by using  $S$  measured at  $E = 0.4$ – $0.5$  keV. The error bar is close to the size of the symbol. The  $S$  value for crystalline  $\text{Al}_2\text{O}_3$  was 0.415. Thus, the large  $S$  value shown in Fig. 3 indicates the annihilation of positrons trapped by open spaces in the  $\text{AlON}_x$  film. The  $S$  value increases with the increasing size of open spaces and/or their concentrations. Thus, the change in  $S$  can be associated with the change in a weighted average size of open spaces. For the samples with the  $\text{AlON}_x$  film ( $x \geq 3\%$ ), the  $S$  value increases as the annealing temperature increases, which can be attributed to the increase in the average size of open spaces. For the AIO film ( $x = 0\%$ ), however, the  $S$  value starts to decrease above  $800^\circ\text{C}$  annealing, which can be attributed to the shrinkage of the average size of open spaces. These facts indicate that nitrogen incorporation into the AIO film suppresses the shrinkage of open spaces above  $800^\circ\text{C}$  annealing. For  $\text{AlON}_{0.25}$  after annealing above  $800^\circ\text{C}$ , however, the  $S$  values are smaller than those for  $\text{AlON}_x$  with  $x = 3\%$ – $15\%$ , indicating that the effect of nitrogen incorporation on open spaces diminishes at  $x = 25\%$ .

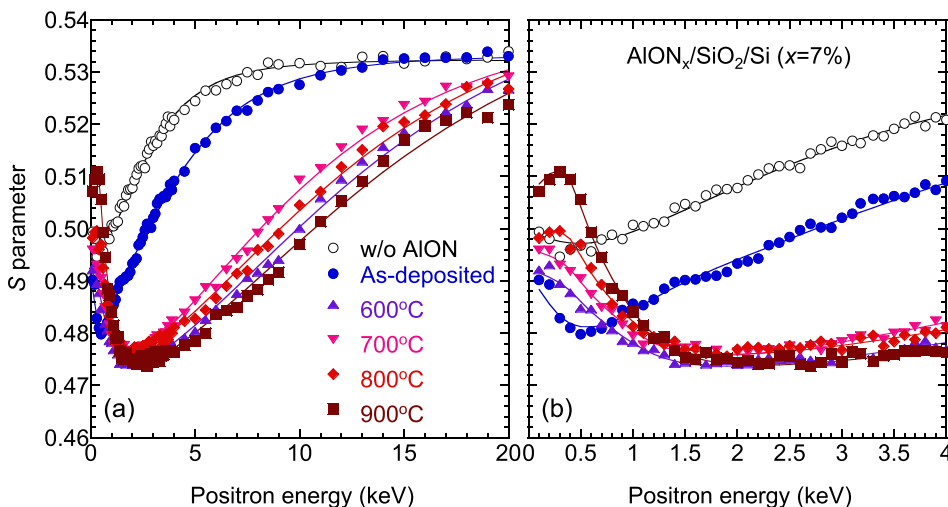


FIG. 2.  $S$  parameters as a function of incident positron energy  $E$  for  $\text{AlON}_{0.07}/\text{SiO}_2/\text{Si}$  samples before and after annealing [(a)  $E = 0.1$ – $20.0$  keV and (b)  $E = 0.1$ – $4.0$  keV]. The result for the  $\text{SiO}_2/\text{Si}$  sample without annealing is also shown.

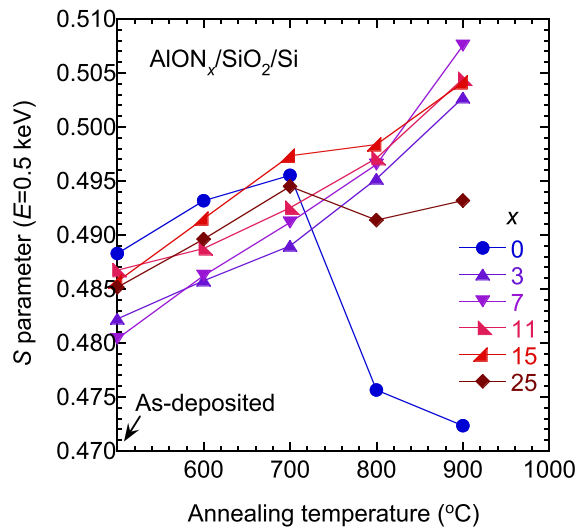


FIG. 3.  $S$  parameter as a function of annealing temperature of  $\text{AlON}_x$  films ( $x = 0\%–25\%$ ). The results for as-deposited samples are also shown.

For  $\text{AlON}_x$  ( $x = 0\%$ ,  $7\%$ , and  $25\%$ ) before and after annealing at  $900^\circ\text{C}$ , the lifetime spectra of positrons were measured at  $E = 0.5$  keV. The spectra were decomposed into three components, and the obtained lifetimes and corresponding intensities are shown in Fig. 4. The error bars of those parameters are close to or smaller than the size of symbol in the figure. The third lifetime ( $\tau_3$ ) indicates the formation of positronium (Ps: a hydrogen-like bound state between a positron and an electron) in  $\text{AlON}_x$ . The  $\tau_3$  value varied from 2.8 to 4.9 ns. According to the relationship between the Ps lifetime and the size of open spaces (or free volume) used for amorphous polymers,<sup>8</sup> the diameters corresponding to this range can be estimated to be 0.7–0.9 nm. The lifetime of

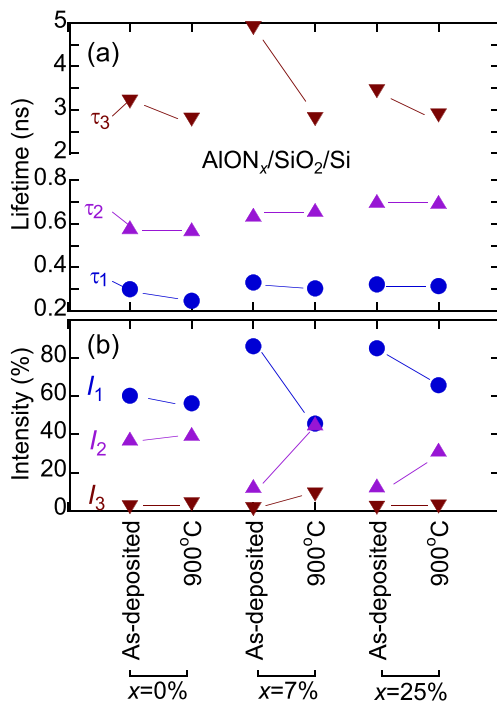


FIG. 4. (a) Positron lifetimes ( $\tau_1$ ,  $\tau_2$ , and  $\tau_3$ ) and (b) corresponding intensities ( $I_1$ ,  $I_2$ , and  $I_3$ ) for  $\text{AlON}_x$  films before and after annealing at  $900^\circ\text{C}$ . Lifetime spectra were measured at  $E = 0.5$  keV.

positrons annihilated from the free state in crystalline  $\text{Al}_2\text{O}_3$  was 143 ps.<sup>15</sup> Because the first and second positron lifetimes ( $\tau_1$  and  $\tau_2$ ) are longer than this value, they can be associated with the annihilation of positrons trapped by open spaces which are smaller than the ones detected by the third component. Thus, one can conclude that open spaces with three different sizes coexist in the as-deposited  $\text{AlON}_x$  film, and this is still true for the films annealed up to  $900^\circ\text{C}$ . Kimoto *et al.*<sup>16</sup> reported that atomic coordinates of the thin  $\text{Al}_2\text{O}_3$  film deposited by atomic layer deposition were close to those of  $\gamma\text{-Al}_2\text{O}_3$ . Consequently, Uedono *et al.*<sup>17</sup> simulated the positron lifetimes in  $\gamma\text{-Al}_2\text{O}_3$ . In a spinel-like  $\gamma\text{-Al}_2\text{O}_3$  structure, since eight Al vacancies ( $V_{\text{Al}}$ s) exist in three spinel unit cells to satisfy stoichiometry, Al atoms were removed from the super cell using random numbers in the simulation. The positron lifetime was obtained in the range between 0.22 ns and 0.26 ns. Here, the lifetime distribution reflects the size variation of open spaces. For example, when positrons are mainly localized in the open space consisting of three  $V_{\text{Al}}$ s, the lifetime was obtained as 0.245 ns. This lifetime is close to  $\tau_1$  for AIO after  $900^\circ\text{C}$  annealing, indicating that the size of open space detected by the first component is close to that of such a vacancy agglomerate.

The  $\tau_2$  value increased as  $x$  increased, indicating that the nitrogen incorporation increased the size of the medium-sized open space in the amorphous network. For the  $\text{AlON}_x$  films with  $x = 7\%$  and  $25\%$ , the  $I_2$  values increase after annealing, and the intensity of the short-lived component ( $I_1$ ) decreases. This behavior is consistent with the observed increase in the  $S$  value after annealing for  $\text{AlON}_x$  (Fig. 3). For the AIO film, however, the change in the intensities is small, and the values of  $\tau_1$  and  $\tau_3$  decrease after annealing. These facts indicate that the nitrogen incorporation suppressed the shrinkage of open space after annealing. For as-deposited  $\text{AlON}_x$  with  $x = 7\%$  and  $25\%$ , however, the  $I_2$  values are smaller than those for AIO, indicating that annealing treatment done at the appropriate temperature is indispensable for nitrogen incorporation to affect the network structure of the film.

Using the positron annihilation technique and x-ray photoelectron spectroscopy (XPS), Uedono *et al.*<sup>18</sup> reported the effect of nitrogen incorporation in 5 nm-thick  $\text{HfSiON}_x$  films deposited on Si substrates. They reported that the average size of open spaces increased as  $x$  increased, and this is mainly due to the increase in the density of Si-N bonds. From the measurements of XPS for  $\text{AlON}_x$  ( $x = 11\%–41\%$ ) deposited on SiC, Takeuchi *et al.*<sup>6</sup> reported that the density of Al-N bonds increased but that the density of Al- $\text{NO}_2$  decreased as the N content increased. In the present experiment, therefore, the formation of Al-N bonds was likely to increase the  $\tau_2$  value. The nitrogen incorporation and the resultant increase in the average size of open spaces are thought to be related to the stabilization of the amorphous structure, which suppresses the crystallization of the AIO film. From this point of view, an appropriate  $x$  value can be determined to be 3%–15% (Fig. 3). Because the nitrogen incorporation effect is strongly affected by the post-annealing temperature, both the nitrogen content and annealing temperature are important process parameters for optimizing the deposition conditions of the  $\text{AlON}_x$  gate insulator.



We used monoenergetic positron beams to characterize  $\text{AlON}_x$  films deposited on the  $\text{SiO}_2/\text{Si}$  stack by using a reactive sputtering technique. Open spaces with three different sizes were detected in the  $\text{AlON}_x$  film, and the volume of medium-sized open spaces was increased by the nitrogen incorporation. After the annealing treatment, the density of the medium-sized open spaces increased for  $\text{AlON}_x$ . The observed increase in the density and size of open spaces was associated with the formation of a stable amorphous structure. The present work indicates that positron annihilation parameters are sensitive to the network structure in the thin  $\text{AlON}_x$  film, and it can provide useful information for process optimization for devices with  $\text{AlON}_x$  insulators.

This work was supported by the Cross-ministerial Strategic Innovation Promotion Program (SIP), “Next-generation power electronics” (funding agency: NEDO). A part of this work was also supported by JSPS KAKENHI (Grant No. 16H06424).

<sup>1</sup>J. Robertson, *Eur. Phys. J.: Appl. Phys.* **28**, 265 (2004).

<sup>2</sup>M. D. Groner, J. W. Elam, F. H. Fabreguette, and S. M. George, *Thin Solid Films* **413**, 186 (2002).

<sup>3</sup>K. Manabe, K. Endo, S. Kamiyama, T. Iwamoto, T. Ogura, N. Ikarashi, T. Yamamoto, and T. Tatsumi, *IEICE Trans. Electron.* **E87-C**, 30 (2004).

<sup>4</sup>Y. Hori, C. Mizue, and T. Hashizume, *Jpn. J. Appl. Phys.* **49**, 080201 (2010).

<sup>5</sup>R. Asahara, M. Nozaki, T. Yamada, J. Ito, S. Nakazawa, M. Ishida, T. Ueda, A. Yoshigoe, T. Hosoi, T. Shimura, and H. Watanabe, *Appl. Phys. Express* **9**, 101002 (2016).

<sup>6</sup>W. Takeuchi, K. Yamamoto, M. Sakashita, O. Nakatsuka, and S. Zaima, *Jpn. J. Appl. Phys.* **57**, 01AE06 (2018).

<sup>7</sup>R. Krause-Rehberg and H. S. Leipner, *Positron Annihilation in Semiconductors, Solid-State Sciences* (Springer-Verlag, Berlin, 1999), Vol. 127.

<sup>8</sup>*Principle and Application of Positron and Positronium Chemistry*, edited by Y. C. Jean and D. M. Schrader (World Scientific, Singapore, 2003), p. 167.

<sup>9</sup>K. Watanabe, M. Nozaki, T. Yamada, S. Nakazawa, Y. Anda, M. Ishida, T. Ueda, A. Yoshigoe, T. Hosoi, T. Shimura, and H. Watanabe, *Appl. Phys. Lett.* **111**, 042102 (2017).

<sup>10</sup>A. van Veen, H. Schut, M. Clement, J. M. M. de Nijs, A. Kruseman, and M. R. Ijpma, *Appl. Surf. Sci.* **85**, 216 (1995).

<sup>11</sup>P. Sperr, W. Egger, G. Kögel, G. Dollinger, C. Hugenschmidt, R. Repper, and C. Piochacz, *Appl. Surf. Sci.* **255**, 35 (2008).

<sup>12</sup>P. Kirkegaard, M. Eldrup, O. E. Mogensen, and N. J. Pedersen, *Comput. Phys. Commun.* **23**, 307 (1981).

<sup>13</sup>K. Iwamoto, Y. Kamimuta, A. Ogawa, Y. Watanabe, S. Migita, W. Mizubayashi, Y. Morita, M. Takahashi, H. Ota, T. Nabatame, and A. Toriumi, *Appl. Phys. Lett.* **92**, 132907 (2008).

<sup>14</sup>K. Kita and A. Toriumi, *Appl. Phys. Lett.* **94**, 132902 (2009).

<sup>15</sup>A. Uedono, K. Ikeuchi, K. Yamabe, T. Ohdaira, M. Muramatsu, R. Suzuki, A. S. Hamid, T. Chikyow, K. Torii, and K. Yamada, *J. Appl. Phys.* **98**, 023506 (2005).

<sup>16</sup>K. Kimoto, Y. Matsui, T. Nabatame, T. Yasuda, T. Mizoguchi, I. Tanaka, and A. Toriumi, *Appl. Phys. Lett.* **83**, 4306 (2003).

<sup>17</sup>A. Uedono, T. Nabatame, W. Egger, T. Koschine, C. Hugenschmidt, M. Dickmann, M. Sumiya, and S. Ishibashi, *J. Appl. Phys.* **123**, 155302 (2018).

<sup>18</sup>A. Uedono, K. Ikeuchi, T. Otsuka, K. Shiraiishi, S. Miyazaki, N. Umezawa, A. Hamid, T. Chikyow, T. Ohdaira, M. Muramatsu, R. Suzuki, S. Inumiya, S. Kamiyama, Y. Akasaka, Y. Nara, and K. Yamada, *J. Appl. Phys.* **99**, 054507 (2006).